Discrete element investigation of stress fluctuation in granular flow at high strain rates

O. J. Schwarz, Y. Horie, and M. Shearer
Department of Civil Engineering, North Carolina State University, Raleigh, North Carolina 27695
(Received 18 August 1997)

The high rate shear of a granular material is investigated by the use of a discrete mesodynamic method. The simulation describes a Couette flow geometry without gravity. A collection of frictional and perfectly smooth particles are subjected to strain rates ranging from $\frac{2}{3}\times 10^1$ to $\frac{2}{3}\times 10^4$ 1/s at solids concentrations ranging from 75% to 87% in a two-dimensional geometry. Normal stresses at the base of the granular sample are recorded. Large fluctuations in individual transmitted stresses are observed. The behavior of this stress profile compares well with previous experimental results. A near linear relation between normal stress and the strain rate is observed. The mechanism of stress transfer, stress chain formation, and random particle collision, through the depth of the sample, is seen to depend on solids concentration. Friction affects both the magnitudes of normal stresses and the characteristics of the granular flow. [S1063-651X(98)13902-8]

PACS number(s): 83.10.Pp, 46.10.+z, 02.70.Ns

I. INTRODUCTION

The rapid flow of granular materials plays an important part in many engineering, geological, and industrial applications. Flowing granular materials exhibit behavioral traits of both solids and fluids and, therefore, cannot be easily explained by conventional theory. Although analogies can be made for the behavior and flow of rapidly sheared granular materials with Newtonian fluids [1], due to inhomogeneities in granular density, stress, and temperature, these analogies are not all encompassing and cannot explain all the properties of granular flow. Likewise, because of the dynamic quality of granular material flow, static solid analysis is similarly lacking. For these (and other) reasons, rapid granular material flow has been a subject of numerous studies over the past several decades.

Considerable research has been done in the area of characterizing and predicting the time-averaged quantities of shearing and normal stresses occurring in a sample at various strain rates and solid concentrations [2–6]. Bagnold [7] observed that normal and shear stresses are proportional to the square of the shear rate when the effects of glancing particle collisions overtake the effects of the dispersing fluid pressure. Bagnold termed this the ''grain-inertia'' regime. Craig, Buckholz, and Domato [8] observed similar results, and gave a simple argument for this squared dependence, stating that both momentum change and collision rate are proportional to the relative velocity between particle layers in a shear flow. Similar dependencies of the shearing and normal stresses on the shear (strain) rate have also been observed experimentally [2,3].

In contrast, in a molecular dynamics simulation of granular flow, it was found under similar conditions that, at large strain rates, the dilatency of the sheared sample leads to a regime where the shear stress is not dependent on the strain rate [9]. Savage and Sayed [3] noted that with increasing solids concentrations the data began to depart from the squared dependence. This was attributed in part to the fact that at high concentrations the chance for enduring particle contact is increased and the effects of friction begin to be felt. Upon inspection of their data, for a given solids concentration, it can be seen that departures from the squared dependence also occur at higher shear rates.

The most common experimental setup used to study granular materials is an annular shear cell apparatus in which the upper (shearing) disk is allowed to translate vertically during testing [2,3,8]. Once the dimension becomes constant, measurements of the gap between the upper and lower disks (height of the sheared specimen) are made during the test, and the solids concentration is then calculated. The solids concentration is controlled for a given shear rate by adding or subtracting weight from the top shearing disk.

The effects of experimental conditions on the behavior of a sheared sample cannot be overlooked and have been commented on often in past literature [1,2,10]. Reference [8] listed a large number of factors that influence stress generation within a sheared sample, such as particle size and shape, particle material properties, the coefficient of restitution, elastic and surface frictional properties of the boundaries, and the amount of material being tested. Differences in these parameters could possibly explain many discrepancies in the results of past research.

Recently, a number of researchers have begun to look at the more microscopic properties and behavior of a shear flow of granular materials, focusing on the mechanism by which individual stresses are transmitted and the variance of their magnitudes about the mean stress.

Howell and Behringer [11] recorded time-dependent stresses at the base of a sheared sample in an annular shear cell similar to that used by other experimentalists [2,3]. The stress-time profile showed that individual stress values (peaks) could vary from the mean normal stress by over an order of magnitude, indicating that these stress fluctuations are in fact not negligible. This is contrary to the results of continuum models which are based on averaging material properties across the sample with the assumption that individual stress fluctuations that occur with time are negligible or statistically insignificant. It was also shown that the normalized spectra of stresses did not show rate dependence.

The transmission of stresses through the depth of the sample and their fluctuation are attributed to the formation of stress chains that occur in a granular material when a dispro-

portionate amount of the normal load is carried by ''chains'' of contacting particles from the top surface to the bottom surface [12]. Visualization of stress chains has been achieved with the use of photoelastic disks or fiber optic strands and polarized light in a two-dimensional (2D) and 3D granular-like assembly for both shearing and static granular particle arrangements [10,11,13,14]. Computer simulations of static systems have also shown the existence of stress chains [12,14]. Liu *et al.* [14] stated that the dominant physical mechanism for the formation of stress chains is the inhomogeneity of granular material packing. With a uniform, homogeneously packed sample, one can hypothesize that nowhere in the sample would the stress significantly exceed the mean applied stress. The sample would behave as a monolithic solid, or statically compressed fluid, equally distributing stresses throughout its volume. The need for further studies into the behavior of granular materials under shear at high strain rates and high solids concentrations considering different boundary conditions and the dynamics of stress fluctuations has been stressed. [4,5,10].

The aim of this paper is to investigate some of the above-described unique aspects of rapidly flowing granular material by means of a new 2D quasimolecular computer code called DM2 (discrete mesodynamic modeling). The simulation described in Sec. II was set up in a manner that allows some comparison with previous works. The DM2 technique is based on the analysis of materials by representing them as a collection or assembly of finite-sized elements. Elements contain specific physical and thermochemical states that evolve during simulation due to interaction with neighboring elements. Material response to external and internal stress is represented by the translation and rotation of these elements and by their changed internal states [15]. The DM2 computer code carries out computations at a user-definable time step, thereby allowing the simulation of very high rates of loading and many multiple contact states between individual elements. DM2 allows solids to be modeled as either single or multielement assemblies. For this simulation, individual grains were represented as single spherical compressible elements. A brief presentation of the preliminary results from this computational study have been presented previously [16]; the current paper will present a complete review of the entire finished work and a comparison with experimental findings.

II. MODEL DESCRIPTION AND SETUP

The complete theory behind and capabilities of the DM2 computer code, including the capability to model chemical reactions, was previously described in detail [15,17,18]. However, those elements of the computer simulation technique that directly apply to the current simulation will be described again here.

Mechanical interparticle interaction is based on the fundamental parameters of central pair potential, elastoplastic shear, viscous friction, tangential viscosity, and dry (Coulomb) friction. A graphical representation of contact forces is shown in Fig. 1. Forces acting on an individual element are determined based on the present and past states of that element. The defined interaction states for an element pair are chemically linked and in contact, in contact but not linked,

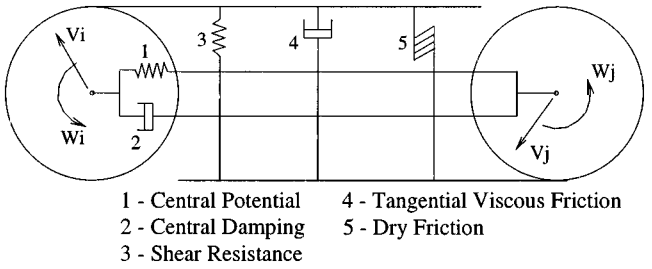

FIG. 1. Element interaction schematic.

linked but not in direct contact, and neither linked nor in contact. In this simulation, elements are modeled as discrete noncohesive particles; therefore, the only governing mechanical contact parameters are a repulsive central potential force and a dry friction force.

Central pair potential force is calculated based on the equation:

$$p_r^{ij}=\frac{\alpha m n}{r_0^{ij}(n-m)}\left[\left(\frac{r}{r_0^{ij}}\right)^{-(n+1)}-\left(\frac{r}{r_0^{ij}}\right)^{-(m+1)}\right], \qquad (1)$$

where p^{ij} is the force of element i on element j, r is the current distance between i and j, and α, m, and n are material constants obtained from fitting the above equation to Hugonial data for a given material. Numerical quantities used in the above and following equations that relate to the modeled material properties are given in Table I. The variable r_0^{ij} is defined by the equation

$$r_0^{ij}=\frac{(d^i+d^j)}{2}, \qquad (2)$$

where d^i and d^j are the undeformed diameters of elements i and j, respectively. Individual elements were modeled to behave elastic perfectly plastically. To simulate the inelastic portion of collisions, a normal component of the viscous friction force is used and defined by

$$f_{vn}=-C_n v_{sn}^{ij}, \qquad (3)$$

where v_{sn} is the normal relative velocity of elements, and C_n is a dissipation coefficient.

Forces resulting from dry friction are calculated from the equation

TABLE I. Material constants for granular material.

elastic modulas	1.429×10^{10} Pa
density	2.4025 g/ce
bulk modulas	8.2126×10^{8} Pa
frictional coefficient	0.2
specific heat	387.2 J/Kg K
element diameter	1.0 mm
α	1.0354×10^{11}
m	1
n	2
calculation time step	2×10^{-8} s (2×10^{-7} s)

$$f_d^{ij} = -u^{ij} p^{ij} t^{ij}, \tag{4}$$

where f_d^{ij} is the dry friction force, u^{ij} is the Coulomb frictional coefficient, p^{ij} is the central force, and t^{ij} is the directional vector.

The internal energy state of an individual element is represented by the element temperature. Energy dissipated from inelastic collision and frictional interaction is considered to go toward an increase in element temperature, and is calculated by

$$\Delta T = \frac{de^i}{C_v^i m^i}, \tag{5}$$

where de^i is the total dissipated energy, C_v^i is the specific heat, and m^i is the mass of element i.

The time increment for calculation was selected based on the limitations posed by DM2's version of the Courant stability condition. Based on this condition, DM2 considers two time increment limitations that deal with particle collision and momentum transfer. First, the time step must be small enough to ensure that colliding elements cannot penetrate each other in one time step. Second, the momentum transferred between two (or more) colliding particles cannot exceed, in a single time step, the total momentum transfer during the entire collision process. The first limitation is based on the parameters of particle velocity and diameter, and the second uses a combination of particle velocity, diameter, and mass. Consideration of this limitation is very important at high loading rates to control momentum transfer at each time step.

Simulations were carried out in a 2D Couette flow geometry of simple shear. The upper and lower boundaries were rigid and consisted of particles of the same size and properties as the sheared granular material (see Table I). The lower boundary remained fixed throughout the simulation and the upper boundary moved with a given velocity in the x direction. Simulations consisted of 559–650 elements, corresponding to solids concentrations ranging from 75% to 87%. Unless otherwise specified, values for solids concentration given from the current simulation were calculated based on the 2D geometry. Values obtained from the literature and given for comparison were 3D solids concentrations, because experimental techniques commonly utilized a 3D shear flow. To facilitate comparison of the behavior of the granular material of this study with that of previous works, the following equation based on interparticle spacing was used [6]:

$$v_{3D} = \left(\frac{4}{3\pi^{1/2}} \right) v_{2D}^{3/2}, \tag{6}$$

where v_{2D} is the 2D solids concentration, and v_{3D} is the 3D solids concentration. Maximum possible solids concentration for the 2D geometry was 88.7%, corresponding to 663 elements. The sheared sample was 1.5 cm deep by 4 cm long. Elements on the left and right boundaries interact with each other to, in effect, form a cylindrical geometry. These conditions were chosen in order to simulate the annular shear cell geometry of many previous experimentalists [2,3,11]. The initial geometry corresponding to a solids concentration of 75% is shown in Fig. 2.

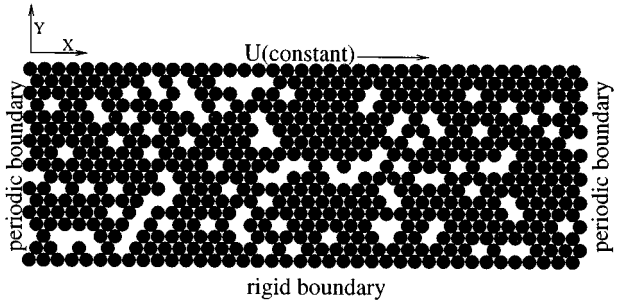

FIG. 2. Initial structure and boundary conditions.

The behavior of both perfectly smooth and frictional granular flows was simulated. Normal stresses at the bottom surface of the sheared region were recorded by a stress gauge consisting of a stationary collection of eight granular elements, as a function of time. Individual particle temperatures and velocities were recorded at given time intervals and were examined based on a spatial average throughout the thickness of the sample in an attempt to characterize the behavior of the sample. The velocity distribution and the intensity of the turbulence were examined as a function of strain rate. Time-averaged and maximum stresses as a function of both strain rate and solids concentration were examined, as were the variances of individual peak stresses from the average.

The DM2 code provides for cubic or close-packed triangular initial element distributions. The sample began from a close-packed triangular geometry, and was sheared to a strain of 66%. A random collection of elements was removed from all samples to reduce the solids concentration. Breaking of the initial structure was usually achieved within the first 10% strain, and the steady state was reached after 33% strain for most samples. The steady state is defined here as the point where the flow properties and transmitted stresses are no longer a direct function of the original particle packing. The steady state is judged by the fact that the original structure is no longer apparent, and the time-averaged transmitted stress through the sample have reached a relatively stable value [16]. By 33% strain, stress gauges placed within the sample had recorded anywhere from 1000 to 20 000 individual stress peaks, giving further evidence that a steady state was reached, similar in manner to arguments of other researchers [4,6]. A representative flow geometry of a sheared sample after having reached a steady state is shown in Fig. 3.

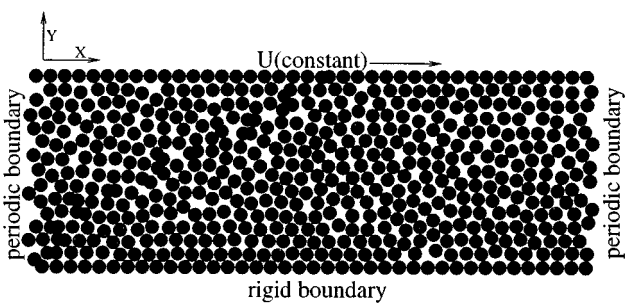

FIG. 3. Sheared structure at 66% strain.

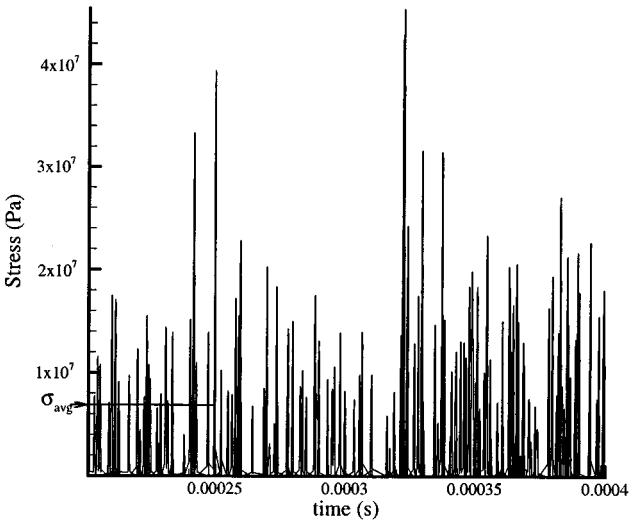

FIG. 4. Stress vs time profile (the strain rate is 3333 1/s).

III. RESULTS AND DISCUSSION

A. Stress transmission and behavior

The stress-time profile obtained from the bottom boundary of the sample undergoing shear at a strain rate of $\frac{1}{3} \times 10^4$ 1/s after it had reached a steady state is shown in Fig. 4. (Profiles from other strain rates show a similar behavior [16].) Individual maximum recorded stresses, at this strain rate, within the steady state region were in the range of 4×10^7 Pa, while the time-averaged stress for this sample was on the order of 7×10^6 Pa. Individual stress fluctuations that exceed the average stress by as much as an order of magnitude have been found experimentally [10], and similar stress fluctuations have been simulated [5]. In their experimental study, Miller, O'Hern, and Behringer [10] attributed the occurrence of such stress fluctuations to the formation of stress chains that carry the majority of the weight of their top bearing plate to the base of the sheared sample. The current computational data were examined for evidence of stress chains at a variety of time steps. However, at a solids concentration of 75% (such as in Fig. 3), no evidence of stress chain formation was found. Instead, the stress peaks that occurred appeared to be due only to the random collision of moving particles in the shear flow. Plots of the flow geometry during a given time span showed only small groups and pairs of stressed elements, without any complete or even semicomplete stress chains (Fig. 5).

If simple intergranular collision is the attributable cause of stress fluctuations, then a theoretical maximum value for transmitted stress can be calculated and compared against the experimental data. Taking into account the collision angle of the grains (elements) in the top shearing layer with the grains immediately below them, the maximum transmitted momentum and/or velocity to the next layer in the vertical direction can be calculated from simple geometry. For a triangularly packed sample, the angle is 60°. Therefore, the vertical component of the velocity vector of the neighboring grain would be

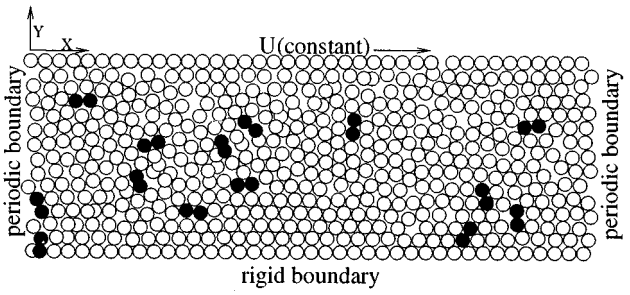

FIG. 5. Flow geometry. Stressed elements are solid.

$$U_p = U \cos^2\left(\frac{\pi}{3}\right), \tag{7}$$

or 75% of the impacting grain's horizontal velocity U. To obtain a maximum value for the transmitted stress, it is assumed, then, that the remaining underlying layers behave as a solid, not a dispersive granular medium. Based on the stress accompanying a compressive shock wave upon collision, this value can then be obtained from the equation

$$\sigma = \rho U_s U_p, \tag{8}$$

where ρ is the density of the material, U_s is the shock wave speed within a given material, and U_p is the impacted particle velocity. Figure 6 shows the maximum normal stress versus strain rate for the theoretical curve and for the experimental data for cases of both smooth and frictional particles at a solids concentration of 75% (50% concentration in three dimensions). (The data point corresponding to the lowest shear rate was not included in this comparison because the time step was set at an order of magnitude larger than that of the other strain rates during its calculation. Omission of this

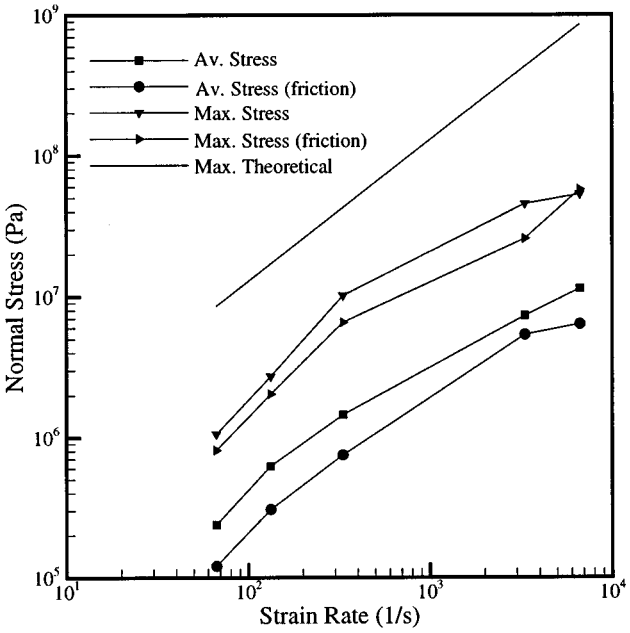

FIG. 6. Average and maximum normal stress as a function of strain rate.

data point was necessitated by a computational limitation; it would have taken roughly ten million time steps to complete the simulation. While the data point corresponding to the maximum normal stress for the strain rate of 6.6 l/s does lie on the same general line with the other data, it was discarded because it could have been artificially elevated due to increased deformation during collision and momentum transfer.)

The predicted maximum stresses were significantly larger than those experimentally measured, but this was anticipated due to assumptions made in the theoretical formulation, which ignored the effect of wave propagation in a granular media. The slope of the experimental line was approximately the same as that of the theoretical curve. This behavior is contrary to previous and predicted experimental results [2,3,7]. However, a departure has been seen from the squared dependence toward a more linear relationship for the stress-strain rate relationship for high solids concentrations, and also for increasing strain rates [3]. Solids concentrations considered by Savage and Sayed [3] varied between 44% and 52%. The 2D solids concentrations of this study, when converted to a comparable 3D value, overlap and exceed the higher range of their experiments, ranging from 50% to 61%. Savage and Sayed [3] hypothesized that deviations from the squared stress-strain rate dependence may be due to effects from enduring interparticle contact, surface friction, and interparticle locking (dead zones in the flow), as well as significant gravitational effects. This does not seem to be the case in the current simulation, however, because no enduring particle contacts were evident, simulations were carried out for perfectly smooth particles, gravity was not introduced into the calculations, and no stagnant zones were apparent in the shear flow (see below). The linear stress strain rate dependence appears to be a function only of the discontinuous transfer of momentum due to interparticle collision, especially at 2D solids concentrations less than 0.82. Current simulation results may also differ from previous experimental results due to the lack of gravitational forces.

Data for the average stresses as a function of strain rate are also plotted on Fig. 6, and follow the same trend as the maximum and theoretical lines. Previous researchers [2,3] measured the stress required to suspend a weighted top plate in an annular shear cell apparatus at a given height. These data are plotted for comparison because the average stress value for the present case, taken over the steady state portion of the stress-time plot, with vertically immobile ''plates,'' should be roughly analogous. When the data of Savage and Sayed [3] were redimensionalized by multiplying their values for stress by particle density, gravity, and particle diameter for spherical polystyrene beads, the data were found to lie on a line roughly two orders of magnitude below the current stresses for any given strain rate. The current individual gauge elements cover a unit area of 1 mm^2 each. The time-averaged stresses were not averaged over the entire gauge area of 8 mm^2. Typically, only one stressed element making up the gauge ''fires'' at a given time, thus it is arguable that average stress was influenced by the size of the gauges used. Also, the juxtaposition of these two data sets for maximum and average normal stress further illustrates the magnitude of individual stress fluctuations compared to the average stress as previously described above. It should also be noted that the standard deviation on the average values (Fig. 6) were generally of the same order of magnitude as the average values themselves, again emphasizing the wide fluctuation of normal stresses.

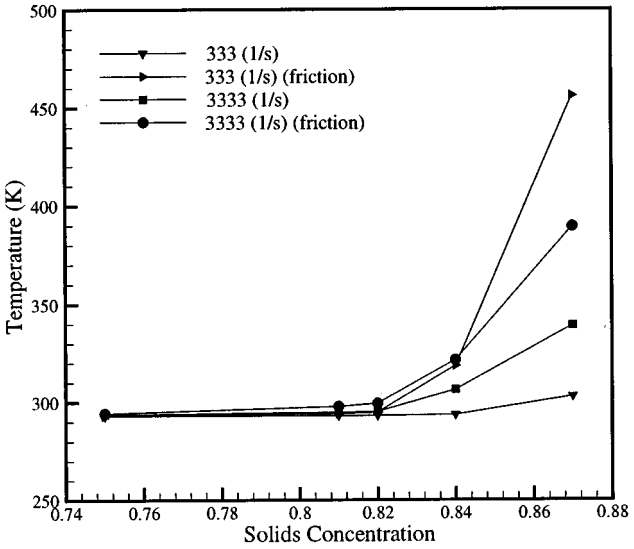

FIG. 7. Granular temperature averaged through the sheared sample as a function of solids concentration (two dimensions) for the given strain rates.

Maximum and average normal stresses for simulations considering friction between particles generally were below those for perfectly smooth particles. It has been similarly noted that with increasing coefficient of friction between particles a subsequent decrease in particle stresses was found [4]. Although only two different cases were simulated in the current study, the data seem to point to the same trend. It would be possible in the future to increase the frictional coefficient and fully compare results. Particle friction also has an effect on the flow properties of granular material under high rates of shear, acting as a ''virtual viscosity,'' damping out turbulence in much the same manner as it seems to damp the magnitude of normal stresses. This point will be discussed in more detail later in this paper.

Granular temperature averaged over the bulk of the sheared sample was relatively constant for a given strain rate at solids concentrations below 0.82. Above this solids concentration, the average sample temperature became increasingly dependent on the solids concentration and experienced a rapid increase for solids concentrations above approximately 0.83 (0.57 for 3D concentrations). The sample temperature as a function of the solids concentration for specified strain rates is shown in Fig. 7. (Other strain rates show the same behavior.) Lun and Bent [4] observed microstructural formation and considerable discrete jumps in individual element stress, temperature, and spin at a solids concentration above approximately 0.52. Such a discontinuous change in the behavior of the normal stresses as a function of solids concentration for the current simulation can also be seen in Fig. 8. The values for the average (and maximum) normal stresses for a given strain rate began to increase dramatically with solids concentration at values above approximately 0.83. It has been shown that at a certain solids concentration, the magnitude of average normal (and shear) stresses begin

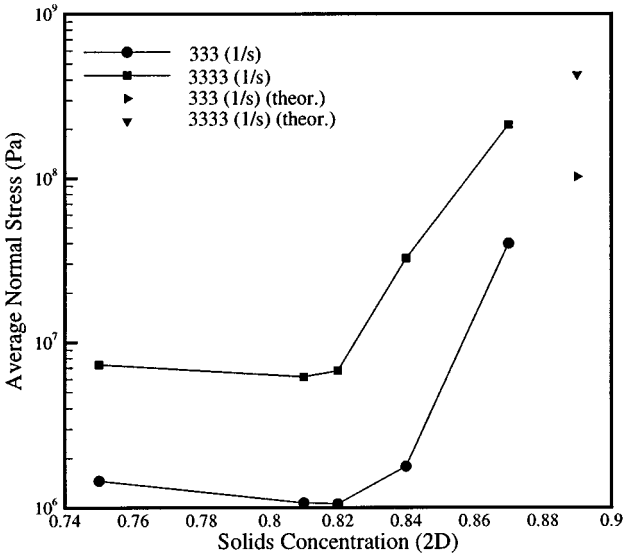

FIG. 8. Normal stress as a function of solids concentration (two dimensions) for the given strain rates. (Maximum theoretical points also plotted.)

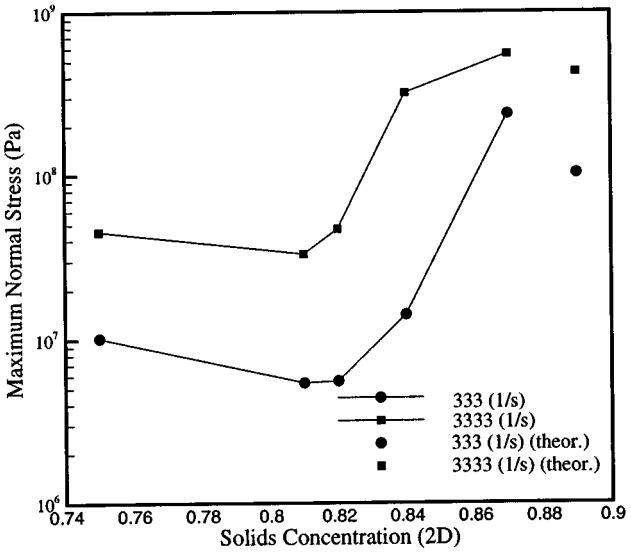

FIG. 10. Maximum normal stress as a function of solid concentration at given strain rates compared to the proposed maximum theoretical stress.

to increase dramatically: for 3D experiments, ''magic'' solids concentrations were approximately 0.54 [2], 0.25 [4], and 0.2 [5]. It should be noted that the value 0.54 was obtained experimentally, and the values of 0.25 and 0.20 were obtained computationally.

The dependence of temperature and stress on the solids concentration points to a distinct change in the physical behavior of the sheared sample. Upon examination of computational data at solids concentrations above 0.82, large numbers of stressed elements were found, forming stress chains linking the top shearing boundary to the bottom boundary at any given time step. Figure 9 shows the geometry of a sample at a solids concentration of 0.84. Because a large number of elements were under stress, the image was cleaned to clearly demonstrate the ''chains'' of concentrated stress. Only those elements having a stress comparable to an order of magnitude greater than or equal to 1×10^7 Pa are shown. Howell and Behringer [11] noted increased stress chain formation in their 2D ''gravity-free'' experiment for solids concentrations within a range of approximately 5%. Current simulation data also shows a possible region for stress chain formation occurring within a range of approximately 3–5 % also. A simplistic boundary condition for the formation of stress chains in a granular material undergoing simple shear can be defined as a state in which the solids packing does not allow particles to easily flow around each other, but instead causes them to be ''ground'' between the top and bottom layers of flow at high local concentrations of solids.

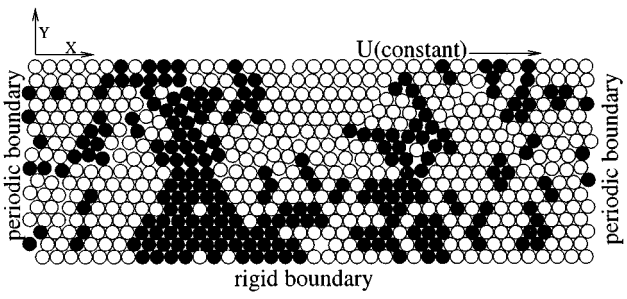

FIG. 9. Flow geometry. Stressed elements are solid. The solids concentration is 0.84.

Miller, O'Hern, and Behringer [10] noted that the common length of stress chains was roughly equivalent to the depth of the sample, i.e., stress chains formed and grew mostly perpendicular to the boundaries. Applying this statement to the current simulation, and assuming that stress chains are caused by the ''grinding'' of particles between the two boundaries, it is possible to hypothesize a relationship for the maximum stress using simple stress-strain relations and the material's elastic modulas. At any given strain rate, then, the maximum possible normal stress, assuming that the sample is of a solids concentration where stress chain activity is possible, is a simple linear addition of the collisional stress and the stress caused by elastic deformation of particles being ''ground'' between the boundaries. Figure 10 shows a comparison of the theoretical estimate of maximum stresses with those of the model simulation as a function of solids concentration.

B. Flow characteristics and structure

The velocity fields of the granular shear flow were examined with respect to strain rate for a solids concentration of 0.75. Velocity profiles for both the translational and normal components of flow were obtained by a spatial average through the sample length, yielding a velocity profile through the depth of the sheared sample. In an attempt to quantify the physical properties of the flow and highlight the effects of frictional particles, the intensity of turbulence was calculated as a function of strain rate and friction.

Shearing through the entire depth of the sample was achieved for all strain rates. A dead, or locked, zone of par-

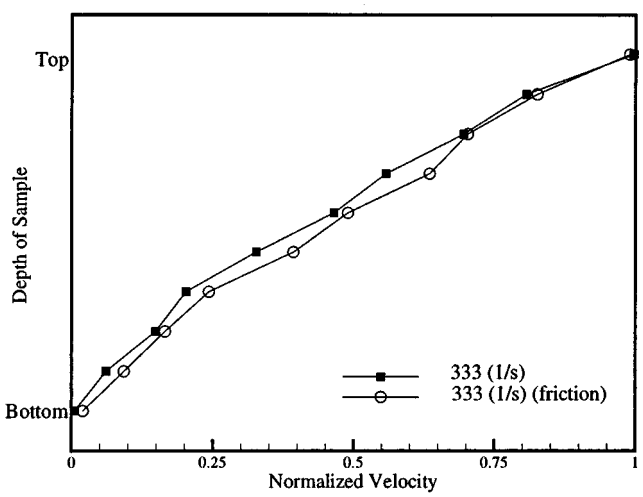

FIG. 11. Normalized velocity through the depth of the sheared sample. The solids concentration is 0.75.

ticles was not observed to occur as it had in many experimental cases [2,3,9]. Transfer of momentum and activity throughout the depth of the sample was likely helped by the absence of gravitational effects. However, at the highest strain rates simulated ($\frac{1}{3}$ and $\frac{2}{3}\times 10^4$ l/s), the top layer appeared to break away from the subsequent layer: while the sample still underwent shear, there was a localized region of higher shear rate near the top surface, similar to that found experimentally [6]. A plot of normalized velocity in the direction of flow (x) through the depth of the sample is shown in Fig. 11 for a representative sample of strain rates. This linear distribution of velocity throughout the depth of the sheared sample was indicative of laminar flow, and generally resembled the Blasius solution for laminar boundary flow [19]. Consideration of frictional particles did not change the general behavior of the sample with respect to the velocity in the direction of flow (Fig. 11). Individual particle velocity vectors for both smooth and frictional particles are shown in Fig. 12. Particles, at this solids concentration, seem to align themselves into layers, allowing for easier flow (Figs. 3 and

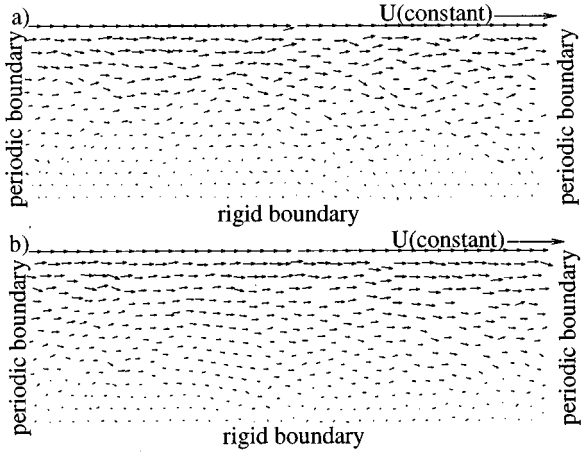

FIG. 12. Particle velocity profile. (a) Smooth particles. (b) frictional particles (the strain rate is 66.7 1/s).

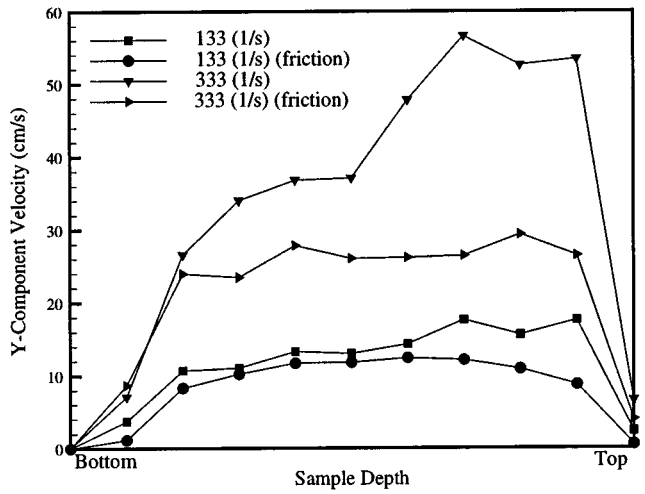

FIG. 13. Spatially averaged vertical component of particle velocities for smooth and frictional particle flows. The solids concentration is 0.75.

12), especially near the top and bottom of the sheared sample. A distinct difference with respect to the vertical components of velocity is apparent from this figure when comparing the smooth and frictional particle flow. Interparticle frictional interaction seemed to damp out the vertical components of velocity and make the flow tend to a more laminar state. Therefore, with an increased frictional coefficient, one would expect that the normal stresses at a given strain rate would likewise decrease, as mentioned earlier in this paper. This trend was apparent at all strain rates considered. Figure 13 further illustrates the effect of friction by showing the spatially averaged vertical component of particle velocities for smooth and frictional particle flow at a given strain rate (these curves have not been normalized).

Analysis of the turbulence of flow based on a defined Reynolds number is difficult, if not meaningless, due to the vast inhomogeneities of the flow in the areas of grain temperature, bulk density, and effective viscosity [20]. Therefore, to quantify the differences in smooth and frictional particle flow as a function of strain rate, the intensity of turbulence was calculated for each case [21] using the formula

$$I=\frac{\sqrt{\frac{1}{3}\overline{u'^2}\,\overline{v'^2}\,\overline{w'^2}}}{\overline{u}}, \tag{9}$$

where I is the intensity of turbulence, u is the average velocity in the direction of flow, and u', v', and w' are the time-averaged average deviations from the average flow in the x, y, and z directions, respectively, at a stationary sampling point. To apply this definition to the current simulation, the equation was modified to two dimensions:

$$I=\frac{\sqrt{\frac{1}{2}\overline{u'^2}\,\overline{v'^2}}}{\overline{u}}. \tag{10}$$

The averaged deviations were obtained spatially instead of over time due to the manner in which data were recorded.

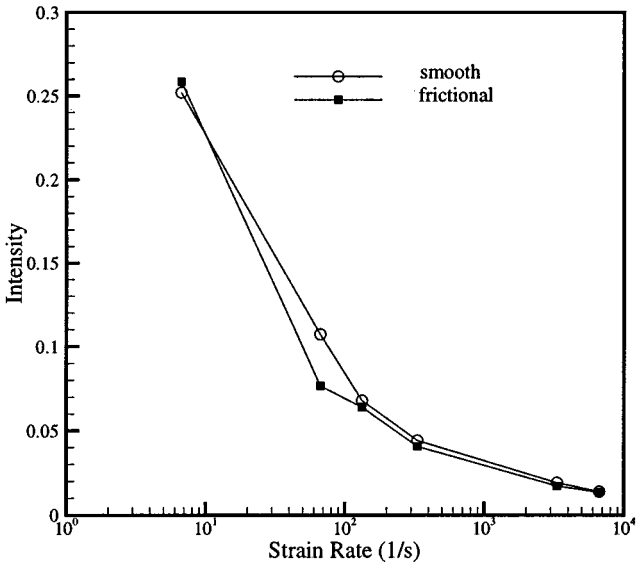

FIG. 14. Intensity of turbulence as a function of the strain rate for smooth and frictional particle flows. The solids concentration is 0.75.

Since the sample models a continuous cylindrically sheared geometry, it can be argued that a spatial average will contain the same statistical data as a time average because the velocity at a point will move through any stationary sampling point with time. Figure 14 shows the turbulence intensity as a function of strain rate for both smooth and frictional particle flows. The intensity is seen to have decreased dramatically with increasing strain rate. Frictional particle interaction also decreased turbulence intensity for a given strain rate, with the exception of the lowest strain rate simulated.

IV. CONCLUSIONS

The behavior of both perfectly smooth and frictional granular flows was investigated at high strain rates and high solids concentrations. Normal stresses at the bottom surface were found to be caused both by random collision of sheared particles and by formation of stress chains at high solids concentrations. Normal stress was related to strain rate at a solids concentration of 0.75. With increasing solids concentrations, maximum and time-averaged normal stresses approached values predicted by a simple theory taking into account collisional stress with a linear addition of stress due to elastic deformation of ''ground'' particles in stress chains. In all cases, friction reduced the magnitudes of transmitted normal stress by seeming to act as a ''virtual viscosity.''

Individual particle temperatures and velocities recorded at given time intervals and examined based on a spatial average throughout the thickness of the sample indicated that a critical or ''magic'' solids concentration exists at which the behavior of the sample, and vehicle for transmission of momentum and stresses, changes from one of simple interparticle collision to one of enduring contacts and stress chain formation. This may be comparable to previous experimental work that observed discrete jumps in stress, temperature, and particle rotation above certain solids concentrations.

The results of velocity distribution and intensity of turbulence as a function of strain rate support the argument that friction between particles damps out stress fluctuation and flow turbulence. However, further study is required to clarify the relation between increasing frictional coefficient and stress at various strain rates.

ACKNOWLEDGMENTS

The authors would like to thank Dr. R. Clelland for his valuable input and comments, R. Schwarz for her time and effort, and K. Yano for his help during numerous discussions concerning this project. This work was supported in part by the U.S. Army Research Office under Grant No. DAAH04-95-1-0269.

[1] D. G. Wang and C. S. Campbell, J. Fluid Mech. **244**, 527 (1992).
[2] D. M. Hanes and D. L. Inman, J. Fluid Mech. **150**, 357 (1985).
[3] S. B. Savage and M. Sayed, J. Fluid Mech. **142**, 391 (1984).
[4] C. K. K. Lun and A. A. Bent, J. Fluid Mech. **258**, 335 (1994).
[5] S. B. Savage, in *Physics of Granular Media*, edited by D. Bideau and J. Dodds, (Nova, New York, 1991), pp. 343–362.
[6] C. S. Campbell and C. E. Brennen, J. Fluid Mech. **151**, 167 (1985).
[7] R. A. Bagnold, Proc. R. Soc. London, Ser. A **225**, 49 (1954).
[8] K. Craig, R. H. Buckholz, and G. Domoto, J. Appl. Mech. **53**, 935 (1986).
[9] P. A. Thompson and G. S. Grest, Phys. Rev. Lett. **67**, 1751 (1991).
[10] B. Miller, C. O'Hern, and R. P. Behringer, Phys. Rev. Lett. **77**, 1310 (1996).
[11] D. Howell and R. P. Behringer, in *Proceedings of the Third International Conference on Powders and Grains, Durham, 1997*, edited by R. P. Behringer and J. T. Jenkins (Balkema, Rotterdam, 1997), pp 337–340.
[12] F. Radjai, M. Jean, J. Moreau, and S. Roux, Phys. Rev. Lett. **77**, 274 (1996).
[13] G. W. Baxter, in *Proceedings of the Third International Conference on Powders and Grains, Durham, 1997* (Ref. [10]), pp 345–348.
[14] C.-h. Liu, S. R. Nagel, D. A. Schecter, S. N. Coppersmith, S. Majumdar, O. Narayan, and T. A. Witten, Science **269**, 513 (1995).
[15] O. Schwarz, Y. Horie, and K. Yano (unpublished).
[16] O. Schwarz and Y. Horie (unpublished).
[17] Z. P. Tang, Y. Horie, and S. G. Psakhie, in High *Pressure Shock Compression of Solids IV*, edited by L. Davison, Y. Horie, and M. Shahinpoor (Springer, New York, 1997), pp. 143–176.

[18] Z. P. Tang, Y. Horie, and S. G. Psakhie, in *Shock Compression of Condensed Matter-1995*, edited by S. C. Schmidt and W. C. Tau (AIP, New York, 1996), pp. 657–660.

[19] W. H. Li and S. H. Lam, *Principles of Fluid Mechanics* (Addison-Wesley, Reading, MA, 1964).

[20] C. Wang, R. Jackson, and S. Sundaresan, J. Fluid Mech. **308**, 31 (1996).

[21] K. K. Kou, *Principles of Combustion* (Wiley-Interscience, New York, 1986), pp. 412–421.